Frontiers in Health Informatics
ISSN-Online: 2676-7104
www.healthinformaticsjournal.com
2024; Vol 13: Issue 6
Open Access

Exploring Benzoxazole Scaffolds: In-Silico Docking, ADME studies, and Synthesis for Breast Cancer Treatment

Roshani Patel*[a], Arjun Modi [a], Hitesh J Vekariya [b]
[a]Research Scholar, R K University, Rajkot, Gujarat, India.
[b]Professor, School of Pharmacy, R K University, Rajkot, Gujarat, India.

Cite this paper as: Roshani Patel, Arjun Modi , Hitesh J Vekariya (2024) Exploring Benzoxazole Scaffolds: In-Silico Docking, ADME studies, and Synthesis for Breast Cancer Treatment. Frontiers in Health *Informatics*, *13(6)* 1026-1035

Abstract:
Breast cancer is one of the most common cancers in women with more than 2 million cases in 2022, worldwide. Not a single reliable drug therapy has been developed for triple-negative breast cancer and resistance is developed against the established therapy. So, there is need to develop novel therapy for the same. The history deacetylase inhibitors (HDACi) show promises as selective anticancer therapies, as they induce chromatin remodelling and normalize altered gene expression. This project, thus, aims to increase the efficacy of Vorinostat on breast cancer by designing, synthesizing, and evaluating new benzoxazole-based derivatives of the drug. Several molecules were designed by changing the linker with different aromatic cap groups and benzoxazole rings. These were then further subjected to molecular docking and in-silico ADME analyses. These compounds possessed a strong affinity for HDAC6, especially compound 9c, which demonstrated significant antiproliferative activity against MCF-7 breast cancer cell lines with an IC_{50} value of 24.1 µg/ml. The adherence of the compounds to Lipinski's rule showed advantageous pharmacokinetic characteristics, such as high gastrointestinal absorption and good bioavailability. The promising results suggest that these novel benzoxazole-based HDAC inhibitors could be a viable option for targeted treatment of breast cancer. More experimental and clinical research is required to determine their potential as effective therapeutic drugs, primarily in aggressive types of breast cancer such as triple-negative breast cancer.
Keywords: Benzoxazole, Anti-breast cancer, in silico docking, ADME, histone deacetylases, HDAC

1. Introduction

With more than 2 million new cases reported in 2022, breast cancer is the most common cancer among women worldwide and poses a significant financial burden to the already declining public health system [1]. The fact that there is a shortage of available treatments for triple-negative breast cancers and that resistance to existing treatments continues to emerge underscores the need to create novel medicines to introduce new pharmaceuticals into the market [2]. One such small molecule inhibitors are the histone deacetylases inhibitors (HDACi), which activate histone deacetylases to induce chromosomal remodeling and restore dysregulated gene expression that indicates advancement of breast cancer [3].

New targets for cancer drugs are histone deacetylases (HDACs). They cause chromatin condensation by eliminating acetyl groups from lysine residues in histone tails. In eukaryotic cells, the process of regulation of gene expression has primarily been found to be controlled through acetylation of lysine residues within the tails of histone proteins [4,5]. Histone acetyl transferases (HATs) and HDACs work in opposition to one another to regulate the amount of lysine acetylation. Lysine acetylation is recognized increasingly as the universal mechanism of regulation over a vast scope of cellular functions despite the fact that chromatin is the most well-known substrate for the enzymes [6]. The 18 mammalian deacetylase enzymes that are now known fall into two main categories:

NAD^+-dependent sirtuins and Zn^{2+}-dependent HDACs. Zn^{2+} is required for Class I metalloenzymes (HDACs 1–3 and 8), class II metalloenzymes (HDACs 4–7, 9–10), and class IV (HDAC 11) While NAD^+ is required for class III (sirtuins 1–7). In fact, the only HDACs that promote tumor cell proliferation, angiogenesis, and differentiation are Zn2+-dependent ones, particularly class I and class II isozymes [6].

Two drugs, SAHA (Vorinostat) and FK-228 (Romidepsin), have been approved for the treatment of cutaneous T-cell lymphomas, and several HDAC inhibitors are currently under different phases of clinical trials [7]. Hydroxamic acids and benzamides are the two significant families of novel HDAC inhibitors have been identified. All these chemical classes exhibited potent anticancer activity in vivo and inhibited HDAC enzyme activity in vitro. Sadly, the eleven metal-dependent HDAC proteins are non-specifically inhibited by hydroxamic acids [8]. Conversely, class I HDAC proteins are specific inhibitors of benzamides [9]. Even though there is still some debate, a reasonably specific profile would be desired even though pan-inhibitors may generally have more adverse effects.

In recent years, many Vorinostat hydroxamic acid derivatives with various linkers or cap groups have been synthesized. These compounds can have a varied aromatic cap group, vary the size of the linker and be composed of different functional groups or have substituted phenyl rings [10–14]. For example, compound BRD-73954 is a selective inhibitor of HDAC6 and HDAC8 and has a phenyl ring in its linker domain [15]. Other examples that deserve mention are analogues in which the phenyl group has been replaced by aromatic heterocycles, such as indazole, thiadiazol, and benzothiazole derivatives. Some of these compounds were significantly more antiproliferative than Vorinostat in in vitro testing. Liu et al. stated that an indazole analogue of Vorinostat, in which the p-methoxy-phenyl group replaced one of the groups, possessed antiproliferative activity similar to that of Vorinostat against the human breast cancer cell line MCF-7, the human colon cancer cell line HCT116, and the human cervical cancer cell line HeLa [16].

This work focused on synthesizing new analogues of Vorinostat with antiproliferative activity against human breast cancer cell lines. In this regard, new Vorinostat analogs were synthesized by modifying the linker with benzoxazole ring analogs and different aromatic caps **(Figure 1)**. Their binding affinity and pharmacokinetic properties were assessed prior to synthesis. Subsequently, their antiproliferative properties were evaluated to identify potential leads for further investigation.

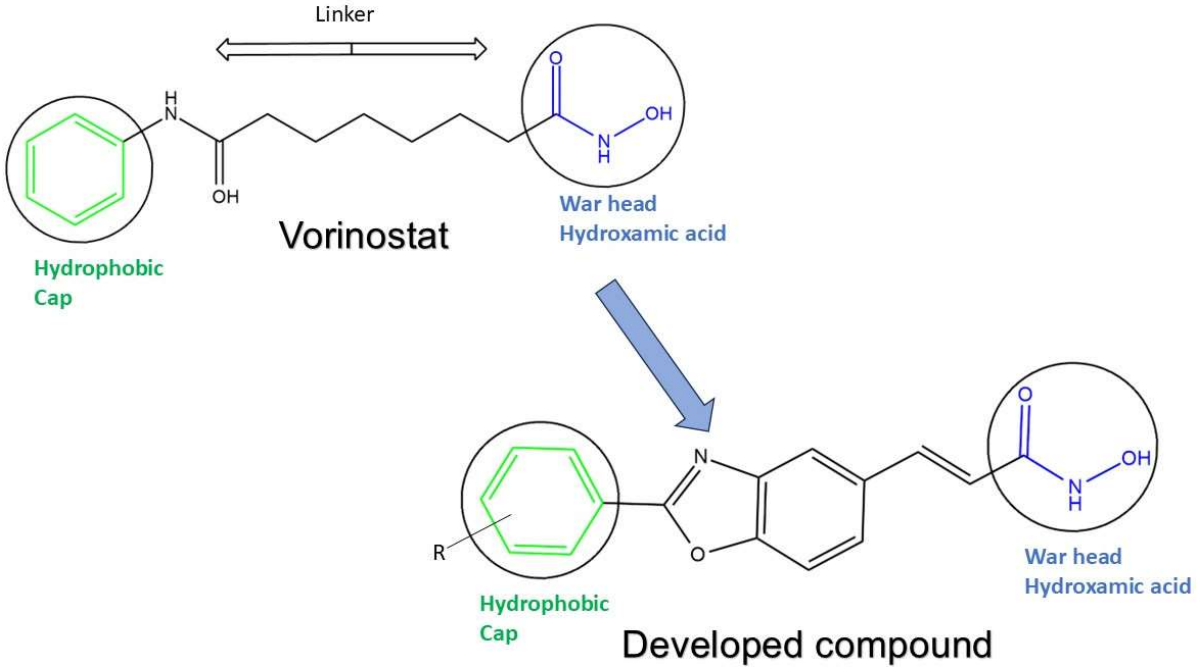

Figure 1: Designing of HDAC inhibitors

2. Chemistry

The synthetic route to obtain the desired compounds is shown in **Figure 2**. Methyl-3-(4-hydroxy-3-nitro phenyl) prop-2-enolate **(3)** is synthesised by refluxing 4-hydroxy-3-nitrobenzaldehyde **(1)** with methyl-2-(dimethoxy phosphoryl) acetate **(2)** in the presence of methanol. The nitro group is then reduced using tin in hydrochloric acid to form methyl-3-(3-amino-4-hydroxy phenyl) acrylate **(4)**. This intermediate is further refluxed with different substituted benzoyl chloride derivatives **(5)** to form intermediates **6a-g**. After hydrolysis, intermediate **7a-g** were obtained, followed by reaction with methylene chloride to yield intermediate **8a-g**. Finally, the intermediate 8a-g was treated with hydroxyl amine to form target compound **9a-g**. ^{1}H NMR was performed by taking DMSO as a solvent. Compound 9a showed singlet at 8.74 δ ppm for hydroxyl and 10.42 δ ppm for amino group of hydroxyl amine, respectively. Similarly, aromatic protons showed multiplet between 7.62 - 8.25 δ ppm while doublets were observed for unsaturated carbon proton at 6.62 and 7.81 δ ppm.

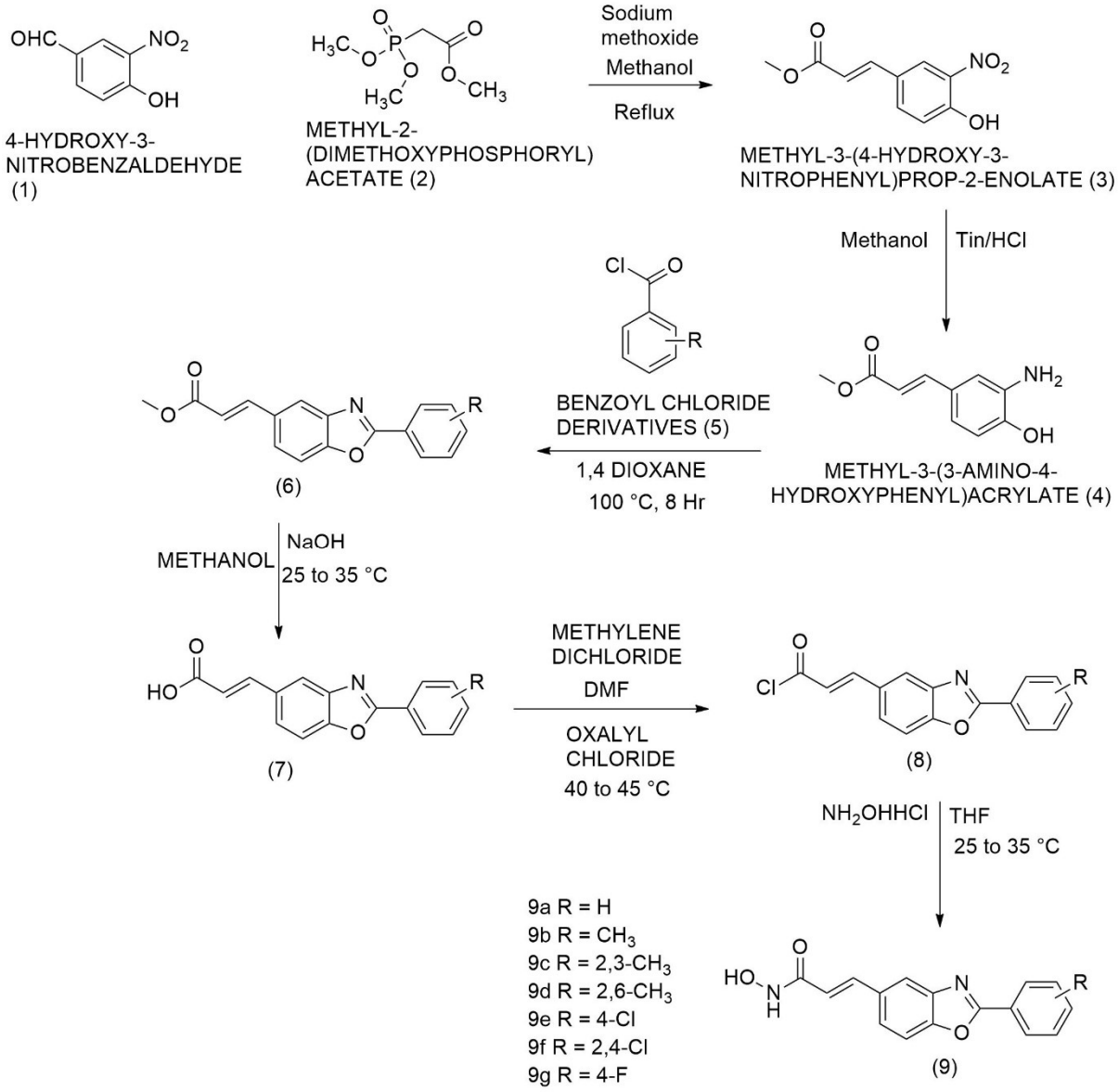

Figure 2: Synthetic methodology of benzoxazole derivatives

3. Materials and Methods

3.1 Materials

All reagents and solvents used in this work were of synthetic grade obtained from Sigma Aldrich, Merk, S D fine, and Loba Chemie. Open glass capillaries melting point (M.P.) apparatus (royal scientific RSW 138 A) was used for the measurement of Melting point of all synthesized compounds and are uncorrected. Progress of the reactions was monitored by TLC (silica gel G plates), using ethyl acetate: hexane solvent system to ascertain the purity of the synthesized compound. Spot on TLC were observed under UV light and/ or by exposing iodine vapours. An NMR Bruker 400 MHz−avance III spectrometer was used to record the ^{1}H-NMR and ^{13}C-NMR spectra, and the chemical shifts were measured in parts per million (ppm). Tetramethyl silane (TMS) was used as the reference Mass and NMR was taken from the Sophisticated Instrumentation Centre for Applied Research & Testing, Anand, Gujarat, India. Finally, all the product was isolated and purified with column chromatography.

3.2 Molecular Docking and in silico ADME Study

Molecular docking was performed using AUTODOCK Vina 2.0, and 2D and 3D visualizations were generated with Biovia Discovery Studio [17]. The protein structure of HDAC6 was obtained from the Protein Data Bank (PDB ID: 6CGP). Both the ligand and protein files were converted into PDBQT format before docking. Water molecules were removed from the protein structure, and only polar hydrogen atoms and Kolman charges were added. A configuration file was created with the following grid box dimensions: center_x = -30.505, center_y = 9.079, center_z = 23.080, and the grid size for x, y, and z coordinates was set to 40. Molecular docking was executed via the command prompt, and binding affinity was calculated in kcal/mol. In-silico analysis was carried out using SWISSADME (http://www.swissadme.ch/) by inserting smiles [18].

3.3 Experimental Procedures

3.3.1 General scheme of synthesis of Methyl-3-(4-hydroxy-3-nitrophenyl)prop-2-enoate (3)

4-Hydroxy-3-nitrobenzaldehyde (1 g, 0.005 mol) was placed in a 100 mL round-bottom flask (RBF). To this, 5 mL of methanol and 0.323 g of sodium methoxide (0.018 mol) were added. The reaction mixture was stirred at 50°C for 30 minutes. After 30 minutes, methyl-2-(dimethoxyphosphoryl) acetate (1.09 g, 0.005 mol) was introduced, and the mixture was stirred at 60°C under reflux. Upon completion of the reaction, the mixture was poured into ice-cold water. The product was then collected and recrystallized using ethanol [19].

3.3.2 General scheme of synthesis of methyl 3-(3-amino-4-hydroxyphenyl)acrylate (4)

In a 125 mL Erlenmeyer flask containing a magnetic stir bar, 2.0 g of methyl-3-(4-hydroxy-3-nitrophenyl)prop-2-enoate and 4.0 g of granular tin were added. Concentrated HCl was dispensed into a 150 mL beaker (40 mL) from the dispensing hood. After the acid was added, the mixture was stirred and heated on a hot plate set to 100°C for 30 minutes, or until most of the tin had dissolved. The reaction mixture was then cooled in an ice-water bath for 10 minutes. Next, 30% (10 M) NaOH was slowly added until the pH reached approximately 10. Methyl-3-(3-amino-4-hydroxyphenyl)acrylate (4) dissolved, leaving SnO as a solid, which was gravity-filtered while hot and washed with hot water. Simultaneously, 25 mL of water was boiled on the hot plate. The filtrate was cooled to room temperature, then placed in an ice-water bath to allow crystallization. This served as a recrystallization of the product from water. Finally, the product was filtered using a vacuum [20].

3.3.3 General procedure of the synthesis of methyl 3-(2-substituted-1,3-benzoxazol-5-yl)prop-2-enolate (6a-g)

Methyl 3-(3-amino-4-hydroxyphenyl) acrylate **(4)** (1 g, 1 mmol) was placed in a 100 mL round-bottom flask (RBF). To this, 6 mL of 1,4-dioxane was added. The reaction mixture was stirred for 10 minutes while cooling (0–5°C). Substituted benzoyl chloride (1.2 mmol) was then added dropwise to the mixture. The temperature was gradually increased, and the reaction was stirred at 100°C for 8 hours. Upon completion of the reaction, the

mixture was poured into ice-cold water. The solid product was collected and recrystallized using ethanol.

3.3.3.1 Methyl 3-(2-phenylbenzo[d]oxazol-5-yl)acrylate (6a)

Yield 45.2 %, mp: 209- 211 ºC; ^{1}H NMR (DMSO-d_6, 400MHz, δ, ppm) δ: 3.78 (s, 3H), 6.63 (d, 1H, J = 16.8 Hz), 7.55-7.78 (m, 3H), 7.83-8.07 (m, 5H), 7.95 (d, 1H, J = 8.0 Hz); MS m/z: 280.3 (M+1).

3.3.3.2 Methyl 3-(2-(p-tolyl)benzo[d]oxazol-5-yl)acrylate (6b)

Yield 52.4 %, mp: 220- 223 ºC; ^{1}H NMR (DMSO-d_6, 400MHz, δ, ppm) δ: 2.23 (s, 3H), 3.79 (s, 3H), 6.63 (d, 1H, J = 16.8 Hz), 7.34 (d, 1H, J = 8.0 Hz), 7.85-8.05 (m, 3H), 7.91-8.15 (m, 4H); MS m/z: 294.3 (M+1).

3.3.3.3 Methyl 3-(2-(2,3-dimethylphenyl)benzo[d]oxazol-5-yl)acrylate (6c)

Yield 48.5 %, mp: 215- 220 ºC; 1H NMR (DMSO-d_6, 400MHz, δ, ppm) δ: 2.21 (s, 3H), 2.25 (s, 3H), 3.78 (s, 3H), 6.64 (d, 1H, J = 16.8 Hz), 7.46 (d, 1H, J = 8.6 Hz), 7.82-7.99 (m, 3H), 7.89-8.13 (m, 3H); MS m/z 308.4 (M+1).

3.3.3.4 Methyl 3-(2-(2,6-dimethylphenyl)benzo[d]oxazol-5-yl)acrylate (6d)

Yield 55.1 %, mp: 215- 220 ºC; ^{1}H NMR (DMSO-d_6, 400MHz, δ, ppm) δ 2.30 (s, 6H), 3.78 (s, 3H), 6.63 (d, 1H, J = 16.8 Hz), 7.15 (d, 1H, J = 8.0 Hz), 7.66-7.93 (m, 3H), 7.78-8.13 (m, 3H); MS m/z: 308.4 (M+1).

3.3.3.5 Methyl -3-(2-(4-chlorophenyl)benzo[d]oxazol-5-yl)acrylate (6e)

Yield 58.7 %, mp: 205- 207 ºC; ^{1}H NMR (DMSO-d_6, 400MHz, δ, ppm) δ: 3.76 (s, 3H), 6.65 (d, 1H, J = 16.8 Hz), 7.78-8.02 (m, 3H), 7.96 (d, 1H, J = 8.5 Hz)), 8.08-8.27 (m, 4H); MS m/z: 313.8 (M+), 315.2 (M+2)

3.3.3.6 Methyl (E)-3-(2-(2,4-dichlorophenyl)benzo[d]oxazol-5-yl)acrylate (6f)

Yield 51.9 %, mp: 190- 195 ºC; ^{1}H NMR (DMSO-d_6, 400MHz, δ, ppm) δ: 3.75 (s, 3H), 6.69 (d, 1H, J = 16.8 Hz), 7.37 (d, 1H, J = 1.8 Hz), 7.85-8.03 (m, 3H), 8.09-8.28 (m, 3H); MS m/z: 347.2 (M+), 349.2 (M+2), 251.4 (M+4)

3.3.3.7 Methyl 3-(2-(4-fluorophenyl)benzo[d]oxazol-5-yl)acrylate (6g)

Yield 52.4 %, mp: 189- 192 ºC; ^{1}H NMR (DMSO-d_6, 400MHz, δ, ppm) δ: 3.77 (s, 3H), 6.68 (1H, d, J = 16.8 Hz), 7.47 (d, 1H, d, J = 8.5 Hz), 7.80-8.05 (m, 3H), 8.08-8.29 (m, 4H); MS m/z: 298.3 (M+1)

3.3.4 General procedure of the synthesis of N-hydroxy-3-(2-(substituted)phenylbenzo[d]oxazol-5-yl)acrylamide (9)

3-(2-(substituted)Phenyl-1,3-benzoxazol-5-yl) acrylic acid **(7a-g)** (1 g, 0.003 mol) was placed in a 100 mL round-bottom flask (RBF), and 2 mL of methylene dichloride (MDC) was added. In a separate RBF, 2 mL of oxalyl chloride and 2 mL of DMF were mixed, and the entire reaction mixture was stirred at 40°C for 1 hour. Next, a saturated sodium bicarbonate solution was added to a mixture of hydroxylamine hydrochloride and tetrahydrofuran (THF, 5 mL) at room temperature, and the reaction was stirred for 15 minutes. The acid chloride compound in THF was then added to the reaction mixture at ambient temperature, and stirring continued for 1 hour, monitoring the reaction by TLC. Upon completion, the product was extracted using a mixture of ethyl acetate and water.

3.3.4.1 N-hydroxy-3-(2-phenylbenzo[d]oxazol-5-yl)acrylamide (9a)

White crystals, yield 73%, mp: 214-216 °C; ^{1}H NMR (DMSO-d_6, 400MHz, δ, ppm) δ: 6.62 (d, 1H, J = 7.6 Hz), 7.81 (d, 1H, J = 6.0 Hz), 7.62 – 7.79 (m, 3H), 7.83 – 8.25 (m, 5H), 8.74 (s, 1H), 10.42 (s, 1H); MS m/z: 281.3 (M+1); Chemical formula: $C_{16}H_{12}N_2O_3$

3.3.4.2 N-hydroxy-3-(2-p-tolylbenzo[d]oxazol-5-yl)acrylamide (9b)

White crystals, yield 76 %, m.p. 182-184°C; ^{1}H NMR (DMSO-d_6, 400MHz, δ, ppm) δ: 2.33 (s, 3H), 6.63 (d, 1H, J = 7.8 Hz), 7.86 (d, 1H, J = 6.0 Hz), 7.62 – 7.79 (m, 3H), 7.84 – 8.24 (m, 4H), 8.74 (s, 1H), 10.43 (s, 1H); MS m/z: 295.3 (M+1); Chemical formula: $C_{17}H_{14}N_2O_3$

3.3.4.3 N-hydroxy-3-(2-(2,3-dimethylphenyl)benzo[d]oxazol-5-yl)acrylamide (9c)

White crystals, yield 75 %, m.p. 172-176°C; ^{1}H NMR (DMSO-d_6, 400MHz, δ, ppm) δ: 2.33 (s, 6H), 6.65 (d, 1H,

J = 7.8 Hz), 7.82 (d, 1H, J = 6.1 Hz), 7.62 – 7.79 (m, 3H), 7.84-8.24 (m, 3H), 8.74 (s, 1H), 10.45 (s, 1H); MS m/z: 309.4 (M+1); Chemical formula: $C_{18}H_{16}N_2O_3$

3.3.4.4 N-hydroxy-3-(2-(2,6-dimethylphenyl)benzo[d]oxazol-5-yl)acrylamide (9d)

Light grey crystals, yield 63 %, m.p. 188-192°C; ^{1}H NMR (DMSO-d_6, 400MHz, δ, ppm) δ: 2.34 (s, 6H), 6.64 (d, 1H, J = 7.6 Hz), 7.82 (d, 1H, J = 6.1 Hz), 7.61 – 7.79 (m, 3H), 7.83 – 8.24 (m, 3H), 8.79 (s, 1H), 10.49 (s, 1H); MS m/z: 309.4 (M+1); Chemical formula: $C_{18}H_{16}N_2O_3$

3.3.4.5 3-(2-(4-chlorophenyl)benzo[d]oxazol-5-yl)-N-hydroxyacrylamide (9e)

Light grey crystals, yield 64.6 %, m.p. 188-192°C ^{1}H NMR (DMSO, 400MHz) δ ppm: 6.64 (d, 1H, J = 7.6 Hz), 7.82 (d, 1H, J = 6.2 Hz), 7.61 – 7.79 (m, 3H), 7.83 – 8.24 (m, 4H), 8.79 (s, 1H), 10.49 (s, 1H); MS m/z: 314.4 (M+), 316.4 (M+2); chemical formula: $C_{16}H_{11}ClN_2O_3$

3.3.4.6 3-(2-(2,4-dichlorophenyl)benzo[d]oxazol-5-yl)-N-hydroxyacrylamide (9f)

Light grey crystals, yield 62 %, m.p. 182-186°C ^{1}H NMR (DMSO, 400MHz) δ ppm: 6.62 (d, 1H, J = 7.7 Hz), 7.82 (d, 1H, J = 6.3 Hz), 7.62 – 7.79 (m, 3H), 7.84 – 8.24 (m, 3H), 8.70 (s, 1H), 10.50 (s, 1H); MS m/z: 349.4 (M+), 351.6 (M+2); Chemical formula: $C_{16}H_{10}Cl_2N_2O_3$

3.3.4.7 3-(2-(4-fluorophenyl)benzo[d]oxazol-5-yl)-N-hydroxyacrylamide (9g)

White crystals, yield 68 %, m.p. > 200 °C, ^{1}H NMR (DMSO, 400 MHz) δ ppm: 6.62 (d, 1H, J = 7.6 Hz), 7.81 – 7.82 (d, 1H, J = 6.2 Hz), 7.62 – 7.79 (m, 3H), 7.84 – 8.24 (m, 4H), 8.70 (s, 1H), 10.50 (s, 1H); MS m/z: 299.3 (M+1); Chemical formula: $C_{16}H_{11}FN_2O_3$

3.4 *In vitro* cell line study

Cell viability of MCF-7 cells was determined using the MTT assay [21]. Cells were seeded in 96-well plates at a concentration of 1×10^4 cells/well and incubated for 24 hours. Then the cells were treated with the compounds (9a–9g) at a range of concentrations from 100 µg/mL to 1.25 µg/mL and incubated at 37°C in 5% CO_2 for 24, 48, or 72 hours. After treatment, 20 µL MTT was added to every well, and the plates were incubated for 2 hours. The solution was removed, and 100 µL DMSO was added to dissolve the formazan crystals. Negative controls contained only culture medium, and cisplatin was used as a positive control. Absorbance was measured at 570 nm (reference: 630 nm), and cell viability was expressed as a percentage of the control. Each compound was determined for its IC50 value.

4. Result discussion

4.1 Molecular docking and *in silico* ADME study

Various molecules were designed by different substitution on phenyl ring. All the designed molecules were then subjected to molecular docking and *in silico* ADME study. The molecules which showed the better affinity and Physicochemical and pharmacokinetic properties were represented in table 1 and table 2, respectively. Also, docking interaction of compound 9c and compound 9e is represented in figure 3(a) and figure 3(b), respectively. Compound 9c exhibited several types of interactions, including π-π, π-alkyl, and hydrogen bonding. The benzoxazole ring formed a π-π interaction with Phe643 and Phe642, while a π-alkyl interaction was observed with Leu712. Hydrogen bonding occurred between the -NH group and the -OH group of hydroxylamine with Gly582. Similarly, compound 9e demonstrated multiple interactions. The benzoxazole ring formed π-π interactions with both Phe642 and Phe643, while the aromatic ring also showed a π-π interaction with Phe642. A π-alkyl interaction was observed between the benzoxazole ring and Leu712. Hydrogen bonding occurred between the -NH group and the -OH group of hydroxamic acid with Gly582. Additionally, a water-mediated hydrogen bond interaction was observed between the -OH group of hydroxamic acid and the HOH903 water molecule.

The molecules demonstrating superior binding affinities were then subjected to in silico analysis. All compounds adhered to Lipinski's rule, indicating that their molecular structure is similar to that of oral drugs. Specifically,

all compounds fall within the established criteria: molecular weight ≤ 500, hydrogen bond donors ≤ 5, topological polar surface area ≤ 140 Å², and hydrogen bond acceptors ≤ 10. Additionally, the log P_o/w values, ranging from 1.53 to 2.95, suggest a preference for partitioning into the water phase. The log S values, indicating aqueous solubility, mostly fall within the desired range of −4 to 0.5 log mol/L, except for compound 9f (Table 2).

Pharmacokinetics plays a vital role in achieving the desired pharmacological effects of a drug. This analysis suggests that the pharmacokinetic properties of these compounds could influence their pharmacological profiles. All derivatives exhibited high gastrointestinal absorption, making them suitable for intestinal uptake. Additionally, all compounds can cross the blood-brain barrier. Regarding drug metabolism, all derivatives were identified as CYP1A2 inhibitors, while compound 9f was also found to inhibit CYP2C19 and CYP2C9, though no effects on CYP2D6 and CYP3A4 were observed. The bioavailability score for all derivatives was 0.55. Furthermore, none of the compounds violated the criteria of the five drug-likeness rules (Lipinski, Veber, Egan, Muegge, Ghose).

Additionally, these derivatives did not raise any PAINS alerts. The Brenk structural alerts identified a few reactive groups in these compounds, including the hydroxamic acid group, Michael acceptor, and oxygen-nitrogen single bond. With molecular weights under 350, these compounds demonstrate lead-like properties. The compounds also achieved synthesis accessibility scores of 3.00 and 3.32, indicating that they can be synthesized through simple, stepwise reactions.

Table 1: Binding affinity and interactions of synthesized molecules(kcal/mol)

Compound	Binding Affinity	Interactions
9a	-9.02	GLY582, PHE642, PHE643, LEU712, HOH903
9b	-8.71	GLY582, PHE583, PHE643, HOH903
9c	-9.53	HIS574, GLY582, HIS614, PHE643, PHE642, LEU712
9d	-8.85	GLY582, PHE642, PHE643, LEU712
9e	-9.21	GLY582, PHE642, PHE643, LEU712, HOH903
9f	-8.63	GLY582, PHE583, PHE643, HOH903
9g	-8.90	GLY582, ALA641, PHE642, PHE643, HOH903

Table 2: Physicochemical and Pharmacokinetic properties

Comp.	HBD	HBA	Log $P_{O/W}$	MW (g/mol)	Log S	MR	Synthesis accessibility	Bioav. Sco.	TPSA Å²
9a	2	4	2.54	280.28	-3.66	78.07	3.03	0.55	75.36
9b	2	4	2.83	294.30	-3.26	83.04	3.17	0.55	75.36
9c	2	4	1.53	308.33	-4.09	88.01	3.32	0.55	75.36
9d	2	4	2.13	308.33	-4.09	88.01	3.32	0.55	75.36

9e	2	4	2.79	314.72	-3.55	83.08	3.00	0.55	75.36
9f	2	3	2.95	349.17	-4.67	88.09	3.08	0.55	75.36
9g	2	5	2.00	298.27	-3.11	78.03	3.02	0.55	75.36

HBD: H-bond donor; HBA: H-bond acceptor; MW: Molecular weight; MR: Molar refractivity; Bioav. Sco.: Bioavailability Score; TPSA: total polar surface area

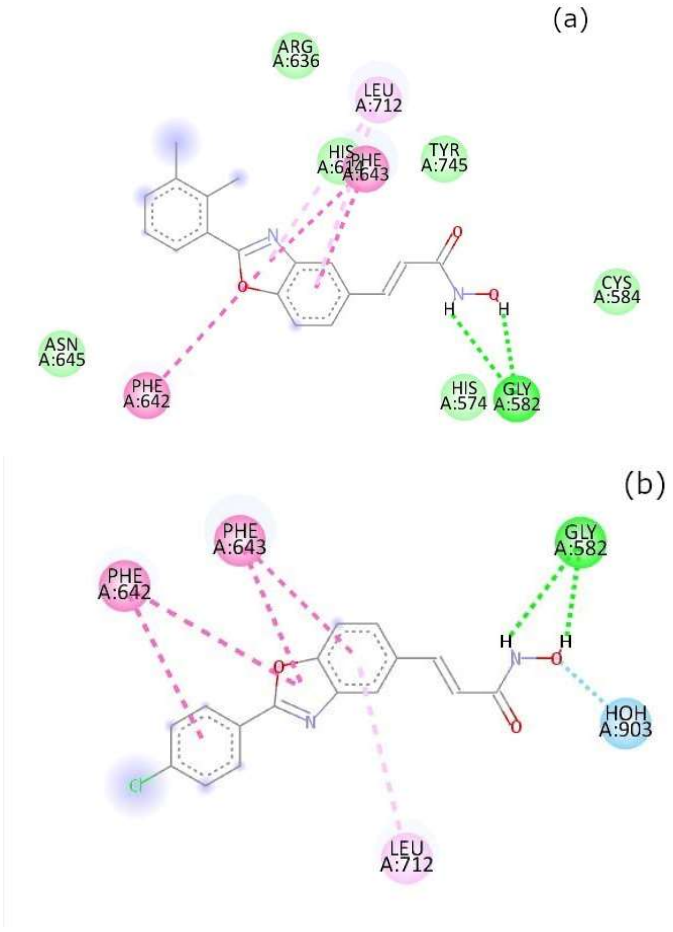

Figure 3: Docking interaction of **(a)** compound 9c **(b)** compound 9e

4.2 *In vitro* Biological evaluation

In vitro anti-breast cancer activity was screened against MCF7 cell lines. The IC_{50} values of compounds 9c, 9e, and 9f were 24.1, 53.4, and 41.7 µg/ml, respectively. The other compounds showed IC_{50} values >80 µg/ml. The compound 9c with dimethyl substitution at 2nd and 3rd position showed the highest activity against anti-breast cancer. However, compounds 9f and 9e, showing dichloro and mono-

chloro substitution, respectively, show moderate activity.

5. Conclusion

The overall design and synthesis of benzoxazole derivatives as novel therapeutic agents against breast cancer, especially via histone deacetylases inhibition, would be of immense interest as a future anticancer agent. Therefore, by altering the analogues of Vorinostat by changing their core to the benzoxazole core, it would not only study molecular docking and ADME properties but also study the in vitro antiproliferative potential of these analogues against human breast cancer cell lines. Various benzoxazole derivatives were designed and subjected to further in-silico studies, ADME predictions, and synthesis, which highlight these compounds as a potential candidate for an anti-breast cancer agent. Synthesised compounds showed potent antiproliferative effects and would be able to target breast cancer cell growth efficiently and inhibit it.

Such research findings are important in how the development of future HDAC inhibitors and other small molecule chromatin remodeling treatments are advanced. These findings provide reasonable evidence for the possibility that benzoxazole-based HDAC inhibitors may serve as a potent therapeutic option in treating breast cancer, particularly in its aggressive forms, like triple-negative breast cancer; however, more experimental, and clinical testing is required. This work gives a strong foundation for further studies and progress in targeted cancer therapy and helps in developing a new line of therapeutic options for breast cancer.

Declarations:

Competing interest

The authors declare that they have no known competing financial interests or personal relationships that could have appeared to influence the work reported in this paper.

Funding

NA

Acknowledgements

None.

References

1. Ibrahim M, Fathalla Z, Fatease AA, Alamri AH, Abdelkader H. Breast cancer epidemiology, diagnostic barriers, and contemporary trends in breast nanotheranostics and mechanisms of targeting. Expert Opinion on Drug Delivery. 2024 Oct 9:1-20. https://doi.org/10.1080/17425247.2024.2412823
2. Subhan MA, Parveen F, Shah H, Yalamarty SS, Ataide JA, Torchilin VP. Recent advances with precision medicine treatment for breast cancer including triple-negative sub-type. Cancers. 2023 Apr 8;15(8):2204. **https://doi.org/10.3390/cancers15082204**
3. Mody D, Bouckaert J, Savvides SN, Gupta V. Rational design and development of HDAC inhibitors for breast cancer treatment. Current Pharmaceutical Design. 2021 Dec 1;27(45):4610-29. https://doi.org/10.2174/1381612827666210917143953
4. Struhl K. Histone acetylation and transcriptional regulatory mechanisms. Genes & development. 1998 Mar 1;12(5):599-606.
5. Witt O, Deubzer HE, Milde T, Oehme I. HDAC family: What are the cancer relevant targets?. Cancer letters. 2009 May 8;277(1):8-21. https://doi.org/10.1016/j.canlet.2008.08.016
6. Choudhary C, Kumar C, Gnad F, Nielsen ML, Rehman M, Walther TC, Olsen JV, Mann M. Lysine acetylation targets protein complexes and co-regulates major cellular functions. Science. 2009 Aug 14;325(5942):834-40. DOI: 10.1126/science.11753

7. Glaser KB. HDAC inhibitors: clinical update and mechanism-based potential. Biochemical pharmacology. 2007 Sep 1;74(5):659-71. https://doi.org/10.1016/j.bcp.2007.04.007
8. Khan N, Jeffers M, Kumar S, Hackett C, Boldog F, Khramtsov N, Qian X, Mills E, Berghs SC, Carey N, Finn PW. Determination of the class and isoform selectivity of small-molecule histone deacetylase inhibitors. Biochemical Journal. 2008 Jan 15;409(2):581-9. https://doi.org/10.1042/BJ20070779
9. Beckers T, Burkhardt C, Wieland H, Gimmnich P, Ciossek T, Maier T, Sanders K. Distinct pharmacological properties of second generation HDAC inhibitors with the benzamide or hydroxamate head group. International journal of cancer. 2007 Sep 1;121(5):1138-48. **https://doi.org/10.1002/ijc.22751**
10. Srinivas C, Swathi V, Priyanka C, Anjana Devi T, Subba Reddy BV, Janaki Ramaiah M, Bhadra U, Bhadra MP. Novel SAHA analogues inhibit HDACs, induce apoptosis and modulate the expression of microRNAs in hepatocellular carcinoma. Apoptosis. 2016 Nov;21:1249-64. https://doi.org/10.1007/s10495-016-1278-6
11. Salmi-Smail C, Fabre A, Dequiedt F, Restouin A, Castellano R, Garbit S, Roche P, Morelli X, Brunel JM, Collette Y. Modified cap group suberoylanilide hydroxamic acid histone deacetylase inhibitor derivatives reveal improved selective antileukemic activity. Journal of medicinal chemistry. 2010 Apr 22;53(8):3038-47. https://doi.org/10.1021/jm901358y
12. Butler LM, Webb Y, Agus DB, Higgins B, Tolentino TR, Kutko MC, LaQuaglia MP, Drobnjak M, Cordon-Cardo C, Scher HI, Breslow R. Inhibition of transformed cell growth and induction of cellular differentiation by pyroxamide, an inhibitor of histone deacetylase. Clinical cancer research. 2001 Apr 1;7(4):962-70.
13. Guan P, Hou X, Wang F, Yi F, Xu W, Fang H. Design, synthesis and preliminary bioactivity studies of 1, 3, 4-thiadiazole hydroxamic acid derivatives as novel histone deacetylase inhibitors. Bioorganic & medicinal chemistry. 2012 Jun 15;20(12):3865-72. https://doi.org/10.1016/j.bmc.2012.04.032
14. Oanh DT, Van Hai H, Park SH, Kim HJ, Han BW, Kim HS, Hong JT, Han SB, Nam NH. Benzothiazole-containing hydroxamic acids as histone deacetylase inhibitors and antitumor agents. Bioorganic & medicinal chemistry letters. 2011 Dec 15;21(24):7509-12. https://doi.org/10.1016/j.bmcl.2011.07.124
15. Olson DE, Wagner FF, Kaya T, Gale JP, Aidoud N, Davoine EL, Lazzaro F, Weïwer M, Zhang YL, Holson EB. Discovery of the first histone deacetylase 6/8 dual inhibitors. Journal of medicinal chemistry. 2013 Jun 13;56(11):4816-20. https://doi.org/10.1021/jm400390r
16. Liu J, Zhou J, He F, Gao L, Wen Y, Gao L, Wang P, Kang D, Hu L. Design, synthesis and biological evaluation of novel indazole-based derivatives as potent HDAC inhibitors via fragment-based virtual screening. European Journal of Medicinal Chemistry. 2020 Apr 15;192:112189. https://doi.org/10.1016/j.ejmech.2020.112189
17. Panchal K, Nihalani B, Oza U, Panchal A, Shah B. Exploring the mechanism of action bitter melon in the treatment of breast cancer by network pharmacology. World Journal of Experimental Medicine. 2023 Dec 12;13(5):142. 10.5493/wjem.v13.i5.142
18. Daina A, Michielin O, Zoete V. SwissADME: a free web tool to evaluate pharmacokinetics, drug-likeness and medicinal chemistry friendliness of small molecules. Scientific reports. 2017 Mar 3;7(1):42717. https://doi.org/10.1038/srep42717
19. A Bisceglia J, R Orelli L. Recent progress in the Horner-Wadsworth-Emmons reaction. Current Organic Chemistry. 2015 May 1;19(9):744-75.
20. Vanderzee CE, Edgell WF. The Kinetics of the Reduction of Aromatic Nitro Compounds with Tin and Hydrochloric Acid1. Journal of the American Chemical Society. 1950 Jul;72(7):2916-23. https://doi.org/10.1021/ja01163a032
21. Ahmadian S, Barar J, Saei AA, Fakhree MA, Omidi Y. Cellular toxicity of nanogenomedicine in MCF-7 cell line: MTT assay. Journal of visualized experiments: JoVE. 2009 Apr 3(26):1191. 10.3791/1191